BioOne COMPLETE

Responses of Alpine Grassland to Climate Warming and Permafrost Thawing in Two Basins with Different Precipitation Regimes on the Qinghai-Tibetan Plateaus

Authors: Zhou, Zhaoye, Yi, Shuhua, Chen, Jianjun, Ye, Baisheng, Sheng, Yu, et al.

Source: Arctic, Antarctic, and Alpine Research, 47(1) : 125-131

Published By: Institute of Arctic and Alpine Research (INSTAAR), University of Colorado

URL: https://doi.org/10.1657/AAAR0013-098

BioOne Complete (complete.BioOne.org) is a full-text database of 200 subscribed and open-access titles in the biological, ecological, and environmental sciences published by nonprofit societies, associations, museums, institutions, and presses.

Your use of this PDF, the BioOne Complete website, and all posted and associated content indicates your acceptance of BioOne's Terms of Use, available at www.bioone.org/terms-of-use.

Usage of BioOne Complete content is strictly limited to personal, educational, and non - commercial use. Commercial inquiries or rights and permissions requests should be directed to the individual publisher as copyright holder.

BioOne sees sustainable scholarly publishing as an inherently collaborative enterprise connecting authors, nonprofit publishers, academic institutions, research libraries, and research funders in the common goal of maximizing access to critical research.

Downloaded From: https://bioone.org/journals/Arctic,-Antarctic,-and-Alpine-Research on 15 Aug 2024
Terms of Use: https://bioone.org/terms-of-use

Arctic, Antarctic, and Alpine Research, Vol. 47, No. 1, 2015, pp. 125–131

Responses of alpine grassland to climate warming and permafrost thawing in two basins with different precipitation regimes on the Qinghai-Tibetan Plateau

Zhaoye Zhou[1,2]
Shuhua Yi[2,5]
Jianjun Chen[2]
Baisheng Ye[2]
Yu Sheng[3]
Genxu Wang[4] *and*
Yongjian Ding[2]

[1]School of Civil Engineering, Lanzhou University of Technology, 287 Langongping Road, Lanzhou, 730050, People's Republic of China
[2]State Key Laboratory of Cryospheric Science, Cold and Arid Regions Environment and Engineering Research Institute, Chinese Academy of Sciences, 320 Donggang West Road, Lanzhou, 730000, People's Republic of China
[3]State Key Laboratory of Frozen Soil Engineering, Cold and Arid Regions Environment and Engineering Research Institute, Chinese Academy of Sciences, 320 Donggang West Road, Lanzhou, 730000, People's Republic of China
[4]Institute of Mountain Hazards and Environment, Chinese Academy of Sciences, No. 9, Block 4, Renminnan Road, Chengdu, 610041, People's Republic of China
[5]Corresponding author:
yis@lzb.ac.cn

Abstract

Alpine grassland and permafrost occupy about two thirds and one half of the total area of the Qinghai-Tibetan Plateau (QTP), respectively. Soil water, which can be affected by permafrost thawing and precipitation, is important for vegetation growth in this region. It is therefore vital to consider the effects of both thawing and precipitation when studying the effect of climate warming on alpine grassland on the QTP. In this study, we examined two adjacent basins, one semiarid and the other semihumid, in the northeastern section of the QTP. We used remote sensing data to compare fractional vegetation cover (FVC) and the relationships between FVC and land surface temperature (LST) in different types of frozen ground; the samples were analogous to a chronosequence of climate warming and permafrost thawing. Our analysis produced three significant results: (1) the FVCs of the semihumid basin were significantly greater than those of the semiarid basin for most types of frozen ground ($p < 0.05$); (2) the changes in FVC along the climate warming and permafrost thawing chronosequence were different in the two basins, with the maximum FVC occurring on the transition permafrost zone in the semiarid basin and on the seasonal frost zone in the semihumid basin; and (3) at the peak of the growing season, only the three warmest types of frozen ground in the semiarid basin had a negative relationship between FVC and LST, suggesting that vegetation growth was limited by water. Therefore, we concluded that the responses of alpine grassland to climate warming in the permafrost regions are complicated by precipitation and permafrost thawing; specifically, grasslands will not necessarily simply degrade as the climate warms, as suggested by previous plot-scale studies.

DOI: http://dx.doi.org/10.1657/AAAR0013-098

Introduction

Permafrost thawing, which is characterized by a thickening of the active layer, rising temperatures in the permafrost, the disappearance of permafrost, and other features, has been reported in different cold regions at high latitudes (e.g., Zhang et al., 1997; Jorgenson et al., 2006). Thawing permafrost may have a significant effect on ecosystem dynamics and carbon cycling (Waelbroeck et al., 1997; Shur and Jorgenson, 2007; Schuur et al., 2009). Alpine grassland is the most common vegetation type on the Qinghai-Tibetan Plateau (QTP). In some parts of the QTP, alpine grassland (primarily alpine meadow and alpine steppe grassland) has degraded over the last few decades (Harris, 2010), leading to the reverse succession of alpine grassland; specifically, a decrease in the number of plant families and species with hygrophytes and mesophytes gradually replaced by mesoxerophytes and xerophytes, the release of soil organic carbon, and a reduction in vegetation cover (Wang et al., 2008; Yang et al., 2010, 2013; Qin et al., 2014). Permafrost occupies nearly half of the total area of the QTP. Over the last few decades, some of the permafrost has thawed (Wu et al., 2006). Therefore, in addition to overgrazing, the thawing of permafrost is considered an important cause of alpine grassland degradation. It is hypothesized that permafrost thawing increases permeability (Niu et al., 2011), causing the water table to drop and shallow soil to dry, thus leading to the degradation of alpine grassland (Wang et al., 2008). Due to the lack of long-term observational studies of alpine grassland dynamics in the permafrost regions of the QTP, most previous studies used the "space-for-time" method to investigate the potential consequences of permafrost thawing, that is, setting up plots on different types of permafrost and treating the spatial differences between the alpine grassland ecosystems as equivalent to chronological changes. The results of these studies supported the above-mentioned hypothesis (Yang et al., 2010). However, due to the difficulties of road accessibility, most of the plots were set close to a road and the representativeness of the plots was poor (Yi et al., 2011).

Yi et al. (2011) used the same "space-for-time" method, but at a basin scale, to investigate alpine grassland vegetation cover in zones with different types of permafrost. Their results showed that vegetation cover increases from the extreme stable permafrost zone (the coldest), is maximized in the transition permafrost zone, and

© 2015 Regents of the University of Colorado
1523-0430/11 $7.00

Downloaded From: https://bioone.org/journals/Arctic,-Antarctic,-and-Alpine-Research on 15 Aug 2024
Terms of Use: https://bioone.org/terms-of-use

then decreases in the warmer soil types. Yi et al. (2011) suggested that this is because different stages of permafrost thawing have different effects on alpine grassland in semiarid basins. Wang et al. (2012) conducted a "space-for-time" study in both semiarid and semihumid regions at a plot scale and found that vegetation cover and biomass decreased in response to permafrost thawing in both regions. However, the reduction was more obvious in the semiarid region than in the semihumid region. Therefore, we hypothesized that the response of alpine grasslands in permafrost regions to climate warming should also be different in contrasting precipitation regimes at a basin scale. To test this hypothesis, we first compared the vegetation covers of alpine grasslands in zones with different types of frozen ground in two adjacent basins with contrasting precipitation regimes; then we compared the relationships between vegetation cover and the remote sensed land surface temperature in each zone.

Methodology

STUDY AREA AND FIELD WORK

The Shule River Basin (hereafter SR) and the Datong River Basin (hereafter DR) are located in the middle of the Qilian Mountains, on the northeastern edge of the QTP, China (Fig. 1). No meteorological station is available in these two basins. SR is in a semiarid region that is characterized by westerly winds. The mean annual air temperature (MAAT) is –2.2 °C, and the mean annual precipitation (MAP) is 309.7 mm, as measured at the nearest Tuole meteorology station (98.42°E, 38.82°N) over the 1981–2010 period. The DR is characterized by westerly winds, southeastern and southwestern monsoons, and more precipitation. Its MAAT and MAP are 1.4 °C and 415 mm, respectively, as measured at the Qilian meteorology station (100.25°E, 38.18°N).

Twenty and eleven boreholes were drilled in the SR and DR, respectively. To determine the frozen ground classification of both basins, the mean annual ground temperature (MAGT) at 15 m was taken from borehole measurements and then the temperatures were related to the topographical characteristics (elevation, aspect, and slope) of each basin; the relationships were extrapolated to get the MAGT at 15 m for each pixel at a 70 m resolution over each basin. Finally, the types of frozen ground were determined based on the MAGT at 15 m (Table 1; Sheng et al., 2010; Li et al., 2012). The spatial distributions of permafrost in the two basins were comparable to those in a previous study by Li and Cheng (1996); there were only two categories in the study area: permafrost and seasonal frost. To our knowledge, these are the only two basins on the QTP with detailed permafrost mapping.

In both basins, the mean elevation and slope generally decrease with the change in permafrost zone from extremely stable, through stable, substable, transition, and unstable to seasonal frost (Table 1). The vegetation types are alpine vegetation, alpine steppe, and alpine meadow on the extreme stable, stable, and transition permafrost zones in both basins; they are alpine steppe and alpine meadow in the SR and DR, respectively, on the other zones (Table 1). Figure 2 shows the differences in the vegetation on the unstable permafrost zones in the two basins. Under dry conditions, alpine steppe is more prevalent than alpine meadow (Yang et al., 2010).

According to the normalized difference vegetation index (NDVI), values produced by a moderate-resolution imaging spectroradiometer (MODIS), vegetation growth peaked between late July and early August in most of the years in the 2001–2011 period (figures not shown here) in both basins. Our field work was conducted between 28 July and 5 August 2011. We set up 25 and 33 plots (30 m × 30 m) in different landscapes that had road accessibility throughout the SR and DR basins, respectively, where the landscape is visually flat and homogenous (Fig. 1). We set nine quadrats (50 cm × 50 cm) in each plot at 15 m intervals (see Yi et al., 2011). We took pictures with a conventional camera and with a multispectral camera (ADC, Tetracam, Chatsworth, California, U.S.A.; 2048 × 1536 pixels.) at a height of about 1.4 m, so that the pictures would cover the whole quadrat.

ESTIMATIONS OF FVC AT A QUADRAT SCALE

A previous study by Yi et al. (2011) accurately estimated the vegetation cover using the WinCAM software (Regent Instruments, Quebec, Canada); however, this method is time-consuming. In this study, we first randomly selected one of the nine quadrats from each plot, and then had two people separately derive the fractional vegetation cover (FVC) from the conventional pictures using the WinCAM software. With the mean of the two FVC values as the target, we calculated the threshold value of the NDVI iteratively, based on the multispectral picture of the same randomly selected quadrat using the following steps: (1) if the NDVI of a pixel in a picture is greater than the threshold value, it is considered a vegetation pixel, otherwise it is a nonvegetation pixel; (2) sum the whole picture to get the number of vegetation pixels, and divide this by the total number of pixels to get FVC; (3) if the FVC is greater than the target value determined from the WinCAM method, then increase the threshold value and vice versa; and (4) iterate through steps 1 to 3 until the difference between the FVC and target value is smaller than 0.01. For more details on this procedure, see Yi et al. (2011). Finally, we calculated the FVC of the other eight quadrats using the calculated NDVI threshold.

FVC AT A 30 M AND A 1 KM SCALE

We used HJ-1A (30 m spatial resolution, 2-day time resolution) data to match the 30 × 30 m plots. HJ-1A is a new generation of Chinese environment satellites that have charge-coupled device cameras with the same bands as the first four bands of a Landsat thematic mapper. We calculated the NDVI with the following equation: $NDVI = (NIR - R)\ (NIR + R)^{-1}$, where NIR and R are the reflectances at the near-infrared and red bands, respectively. The HJ-1A data sets with the highest quality, namely with relatively little cloud cover, were selected from the 29July–5 August period. The 58 plots were partitioned into two categories, one for establishing the relationships between the FVCs measured on the ground and the NDVIs of the corresponding pixels in the HJ remote sensing data, and the other for validating the established relationship. Then we applied the plot scale relationship to the HJ remote sensing data for the whole region in both basins.

We then used the MOD13A2 (NDVI 16-day synthesis) data set to calculate the FVCs at a 1 km scale by (1) resampling the 30-m-scale FVCs to a 1 km scale using the "resample" spatial analyst tool of the ArcGIS 9.3 software; (2) compositing the NDVI images with maximum values from the 28 July–5 August period using the MOD13A2 data set at a 1 km scale; (3) sampling the FVC and NDVI from the field plot locations; (4) establishing the relationship between FVC and NDVI using some of the samples and validating it with the others; and (5) compositing the NDVI images with maximum values for every 16 days between 2001 and 2011, then calculating the FVC with the established relationship at a 1 km scale.

Downloaded From: https://bioone.org/journals/Arctic,-Antarctic,-and-Alpine-Research on 15 Aug 2024
Terms of Use: https://bioone.org/terms-of-use

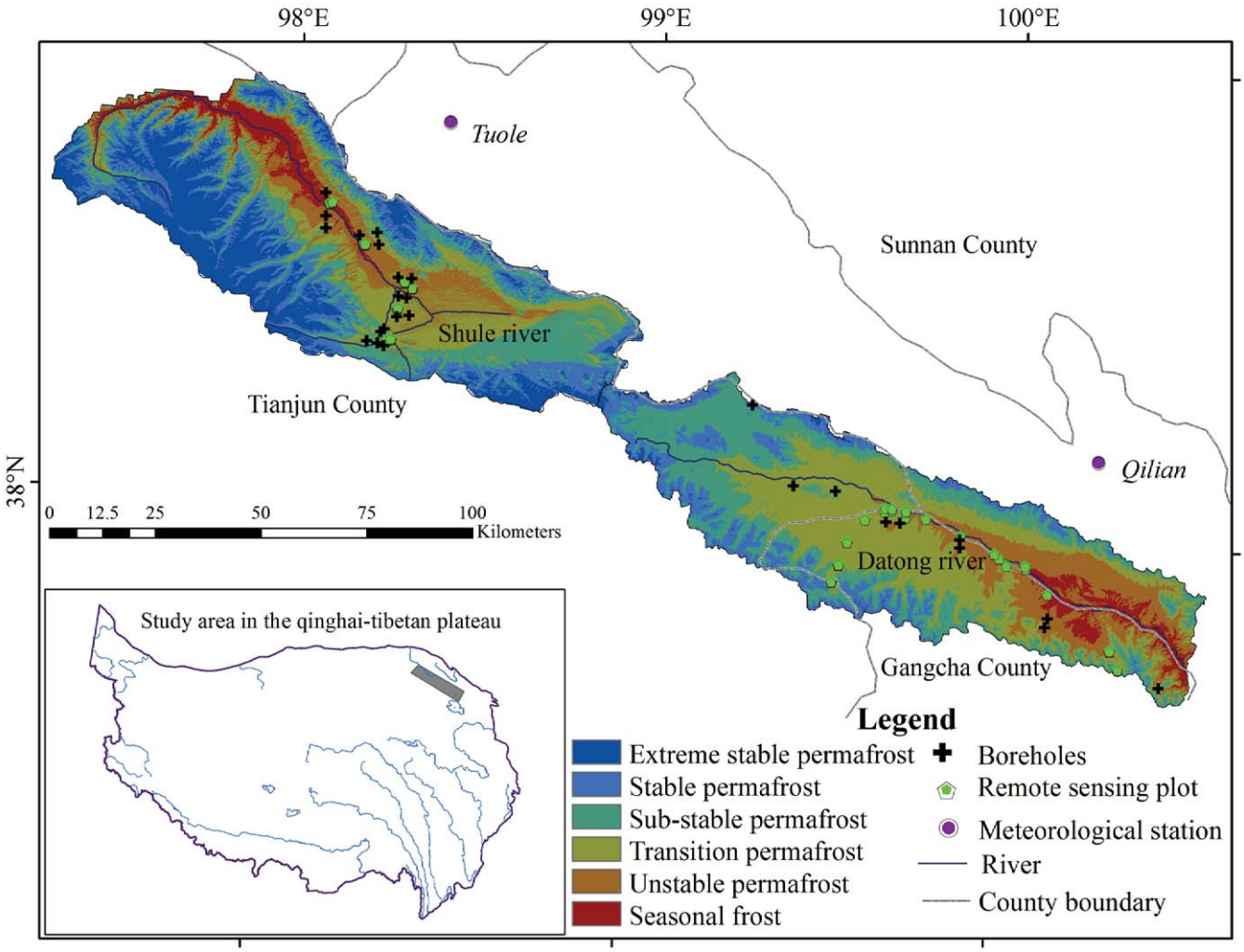

Figure 1. Types of frozen ground and locations of boreholes and remote sensing plots in the semiarid basin (Shule River basin [SR]) and semihumid basin (Datong River basin [DR]). Note: the scale bar is related to the main map.

FIGURE 2. Pictures of the unstable permafrost landscapes of (a) the semiarid basin (SR), which is relatively dry; and (b) the semihumid basin (DR), which is relatively wet.

Downloaded From: https://bioone.org/journals/Arctic,-Antarctic,-and-Alpine-Research on 15 Aug 2024
Terms of Use: https://bioone.org/terms-of-use

TABLE 1

Definition of each type of frozen ground, and the mean elevation and major vegetation type of each type of frozen ground in two basins (SR: Shule River; DR: Datong River). MAGT: mean annual ground temperature at 15 m depth; AV: alpine vegetation; AS: alpine steppe; and AM: alpine meadow.

Frozen ground	Basin	Elevation (m)	Slope (°)	Vegetation type
Extreme stable permafrost	SR	4586	7.55	AV
(MAGT < –5 °C)	DR	4550	7.85	AV
Stable permafrost	SR	4342	5.35	AS
(–5 °C < MAGT < –3 °C)	DR	4293	5.95	AS
Substable permafrost	SR	4141	3.08	AS
(–3 °C < MAGT < –1.5 °C)	DR	4087	2.87	AM
Transition permafrost	SR	3971	1.84	AM
(–1.5 °C < MAGT < –0.5 °C)	DR	3873	1.53	AM
Unstable permafrost	SR	3861	1.78	AS
(–0.5 °C< MAGT < 0.5 °C)	DR	3701	1.62	AM
Seasonal frost	SR	3713	2.59	AS
(MAGT > 0.5 °C)	DR	3592	1.36	AM

Using the 1 km FVC data set, we calculated the FVC statistics for each type of frozen ground and on each basin using SPSS 17.0. As the time series of the FVC samples was too short to be used for climate change studies, we followed previous studies and used the "space-for-time" method, that is, differences in the FVC of different types of frozen ground were used to represent changes in FVC when permafrost is transformed from one type to another. The remote sensing method can only retrieve the aboveground characteristics of vegetation; therefore, we used the term *degradation* to describe the reduction in alpine grassland vegetation cover.

FVC–LST RELATIONSHIPS

Using the 16-day measurements, we created a composite LST from the MOD11A2 (LST 8-day synthesis) data set and a composite NDVI from the MOD13A2 data set. We then calculated the 11-year means of the LST and NDVI at different points in the growing season, which is from 25 May to 14 September. Finally, we compared the relationships between the FVC and LST on different types of frozen ground in both basins.

Results

FVC ESTIMATIONS AT DIFFERENT SCALES

The relationships between the observed FVCs and the corresponding NDVIs from the HJ-1A data set can be described using a linear equation (Fig. 3, part a). The comparisons between the calculated and observed FVCs were reasonably good (Fig. 3, part b). The correlation between FVCs, upscaled from a 30 m to a 1 km scale, and the NDVIs of MODIS are presented in Figure 4, part a. An accuracy test of these data had high precision (Fig. 4, part b). The FVC calculated for different types of frozen ground at a 1 km scale in the two basins showed that in the SR basin, the greatest FVC was in the transition permafrost zone, and that the average FVC in the transition permafrost zone was significantly different from the average FVC in the unstable and substable permafrost zones ($p < 0.05$, Fig. 5). The vegetation cover was minimized on the extreme stable zones, and its average in these zones was significantly different from the average vegetation cover in the stable permafrost and seasonal frost zones ($p < 0.05$, Fig. 5). In contrast, the FVC of the DR basin increased gradually from the extreme stable permafrost through the seasonal frost zones (Fig. 5). Except for the FVCs of the unstable permafrost and seasonal frost zones, there were significant differences between the different types of permafrost zones in the DR. There were significant differences between the two basins for all of the zones except the extreme stable and stable permafrost zones (Fig. 5).

FVC–LST RELATIONSHIPS DURING THE PEAK GROWING SEASON

During the peak growing season, the slopes of the relationships between the FVC and LST in the SR changed from positive in the extreme stable and stable permafrost zones, to relatively weakly positive in the substable permafrost zones, and to negative in the unstable and seasonal frost zones (Fig. 6, part a). In the DR, the slopes altered from positive in the extreme stable and stable permafrost zones, to weakly positive in the other zones (Fig. 6, part b).

Downloaded From: https://bioone.org/journals/Arctic,-Antarctic,-and-Alpine-Research on 15 Aug 2024
Terms of Use: https://bioone.org/terms-of-use

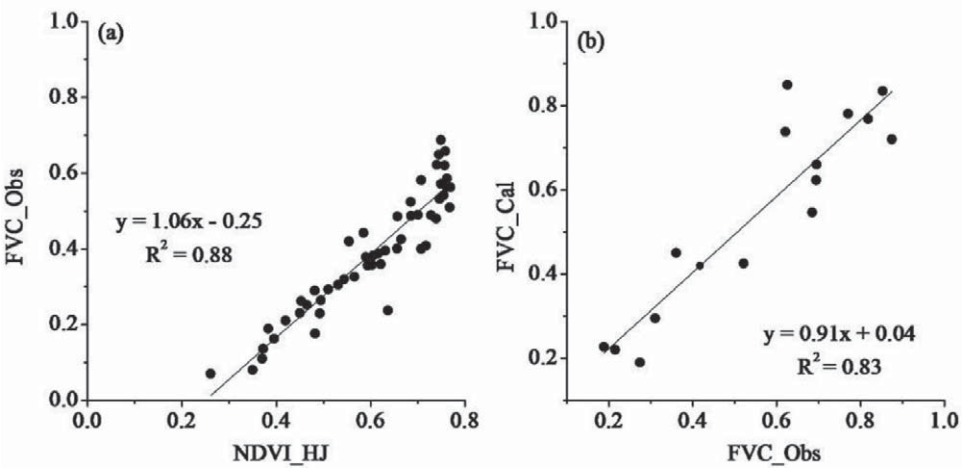

Figure 3. (a) Relationship between fractional vegetation cover (FVC_Obs) and normalized difference vegetation index (NDVI_HJ) at the plot scale (30 m). (b) Comparisons between calculated FVC (FVC_Cal) and observed FVC (FVC_Obs).

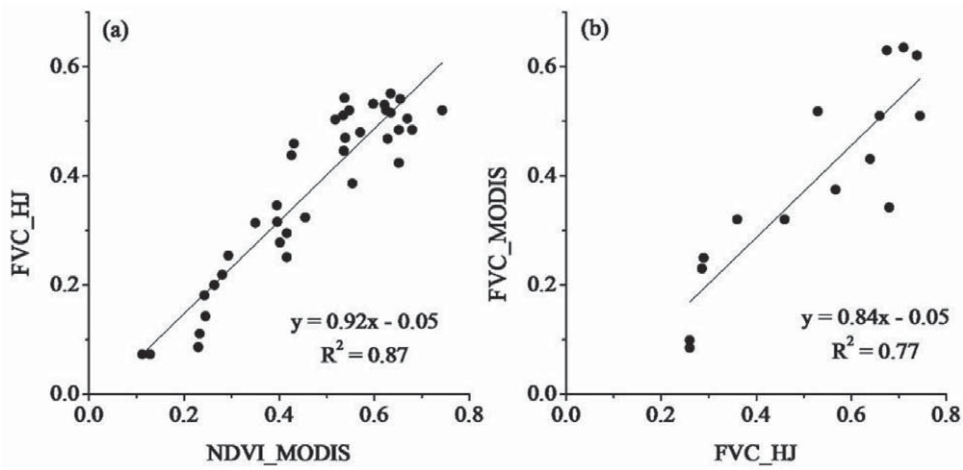

Figure 4. (a) Relationship between fractional vegetation cover (FVC) upscaled from a 30 m scale (FVC_HJ) and the NDVI of a moderate-resolution imaging spectroradiometer (MODIS) (NDVI_MODIS) at a 1 km scale. (b) Comparisons between calculated FVC (FVC_MODIS) and upscaled FVC (FVC_HJ).

SEASONAL VARIABILITY OF THE FVC–LST RELATIONSHIPS

In the SR (Fig. 6, part a), throughout the growing season, the slopes of the relationships between FVC and LST in the extreme stable, stable, and substable permafrost zones were positive, whereas the slopes in the seasonal frost zone were negative or almost zero. For the other types of frozen ground zones, the slopes were positive at the beginning of the growing season, became negative in midsummer, and were positive again at the end of the growing season. In the DR (Fig. 6, part b), the slopes were always positive at the beginning of the growing season, especially in the extreme stable permafrost zone. During midsummer, the slopes were still positive, but less so than at the beginning and end of the growing season.

Discussion

FVCS ESTIMATION AND UPSCALING

FVC is one of the most important characteristics of grasslands. It is widely used in ecological studies as an indicator of vegetation growth (e.g., Wandwei et al., 2013; Yang et al., 2013; Qin et al., 2014). Changes in FVC are minimal within a single day, and even over a few days, especially during the peak growing season. This feature makes FVC a promising variable in ground studies that use remote sensing applications. The challenge is to estimate ground FVC quickly, accurately, and in a nondestructive way and to upscale it to the scales used in satellite remote sensing data sets.

It takes 5 to 10 minutes to derive the "true" FVC using the WinCAM software with a high precision conventional picture (Yi et al., 2011). By using the threshold method, we were able to quickly process a multispectral picture (less than 1 second). In Yi et al. (2011), the FVCs of 10 quadrats, randomly selected from all of the plots, were first estimated based on conventional pictures, then the corresponding NDVI thresholds were calculated, and finally, the average of the 10 thresholds was used as the threshold. However, the pictures were taken at different times of day and on different dates. It is well known that NDVI is affected by solar zenith angle, so it is not accurate to apply an averaged NDVI threshold to multispectral pictures. In this study, we randomly selected one out of the nine quadrats in each plot, determined the NDVI threshold for the quadrat, and applied it to the other eight quadrats. Compared to Yi et al. (2011), our method solved the problem of overestimation for high FVC quadrats and underestimation for low FVC quadrats (figures not shown here).

Downloaded From: https://bioone.org/journals/Arctic,-Antarctic,-and-Alpine-Research on 15 Aug 2024
Terms of Use: https://bioone.org/terms-of-use

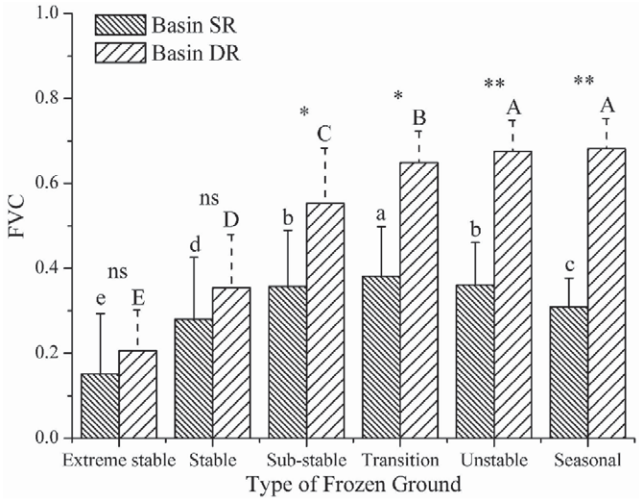

Figure 5. Mean and one standard deviation (error bar) of the fractional vegetation cover (FVC) using the MODIS data set for different types of frozen ground in the semiarid basin (SR) and the semihumid basin (DR). Different letters indicate significant differences ($p < 0.05$) in the FVCs of different types of frozen ground; the lower and upper cases are for SR and DR, respectively; ns, *, and ** indicate no significant differences, significant differences with $p < 0.05$, and significant difference with $p < 0.01$, respectively, in the FVCs of the same type of frozen ground between the two basins.

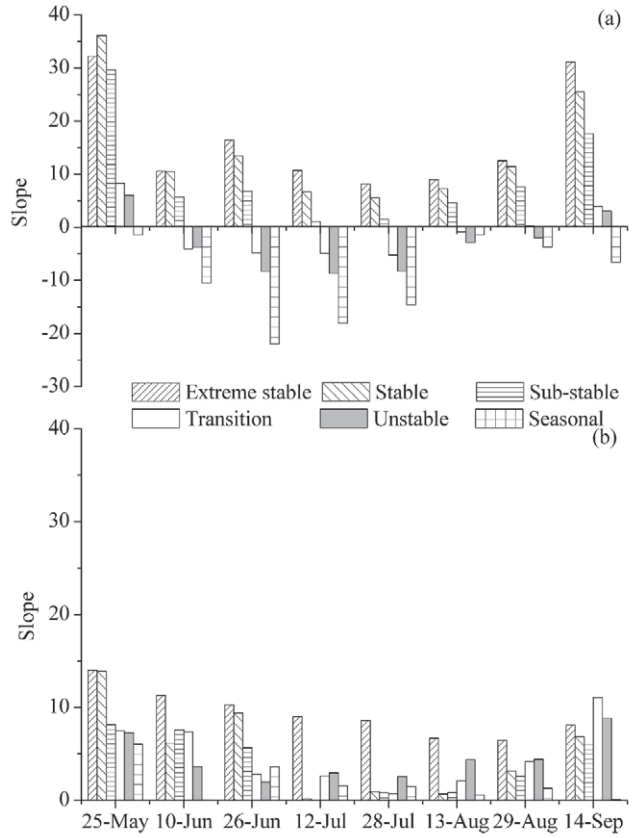

Figure 6. The slope of relationship between the fractional vegetation cover and land surface temperature during the growing season in different types of frozen ground in (a) the semiarid basin (SR) and (b) the semihumid basin (DR).

In this study, we upscaled the FVC from a quadrat scale to a plot scale, and then from a plot scale to a 1 km scale. Traditional methods usually calculate FVC using

$$FVC = (NDVI - NDVI_{min})\,(NDVI_{max} - NDVI_{min})^{-1}, \qquad (1)$$

where $NDVI_{max}$ and $NDVI_{min}$ are the maximal and minimal NDVI of a scene (Barlage and Zeng, 2004). This method has never been tested with ground data. Our method is more suitable.

RESPONSES OF ALPINE GRASSLAND TO CLIMATE WARMING AND PERMAFROST THAWING

According to the traditional "space-for-time" method, climate warming will cause an increase in FVC in extreme stable, stable, and substable permafrost zones in semiarid basins and in most zones in semihumid basins.

The slope of the relationship between FVC and LST can be used to identify the factors that limit vegetation growth, with a positive slope indicating limited thermal energy and a negative slope indicating limited water (Karnieli et al., 2010). In the semihumid basin, the vegetation growth was not limited by water in any of the frozen ground zones during the peak growing season (late July and early August). Furthermore, at the beginning and end of the growing season, vegetation growth was limited by energy. Therefore, future warming would relieve the thermal energy constraint and be conducive to alpine grassland growth. In the semiarid basin, vegetation growth in the transition, unstable, and seasonal frozen zones was limited by water. Vegetation growth in the extreme stable frozen zones in both basins was limited by thermal energy. Therefore, future warming might increase vegetation growth in zones in which vegetation was limited by available thermal energy. However, in zones limited by water, warming would exacerbate water constraints and prohibit alpine grassland growth.

The "space-for-time" method at a plot scale usually focuses on the effects of soil drying (due to warming) on vegetation growth (Baumann et al., 2009; Yang et al., 2010; Wang et al., 2012; Qin et al., 2014). However, drying soil could be partially or fully offset by increased precipitation, and it is likely that warming would also increase nutrient availability and promote vegetation growth (Du et al., 2004; Zhuang et al., 2010). Therefore, the responses of alpine grassland in permafrost regions to warming are complicated by the stages of permafrost thawing and changes in precipitation.

LIMITATIONS AND FUTURE DIRECTIONS

The widely used "space-for-time" method suffers from several shortcomings when used at a plot scale. For example, the study by Qin et al. (2014) had the following limitations: (1) due to limitations in manpower and logistics, only six plots were used; (2) all of these plots were set along roads and no plots were set on stable or extreme stable permafrost zones; and (3) the selected plots did not represent the typical vegetation and soil of a permafrost region. In this study, a combination of field work at a plot scale and remote sensing data was used to retrieve FVC at a basin scale. In future studies, the relationships between other vegetation characteristics (e.g., vegetation

Downloaded From: https://bioone.org/journals/Arctic,-Antarctic,-and-Alpine-Research on 15 Aug 2024
Terms of Use: https://bioone.org/terms-of-use

biomass, community type, etc.) and remote sensing spectral indices should be established to provide more in-depth data at a basin scale. Both temperature and precipitation play an important role in alpine grassland growth. Changes in both temperature and precipitation may occur together. This study only investigated the effects of thawing permafrost, without considering changes in precipitation. To quantify further the responses of alpine grassland to climate change (both temperature and precipitation) and permafrost thawing, it is desirable to use a process-based ecosystem model (e.g., Zhuang et al., 2010). The thawing of permafrost is a consequence of climate warming; but the thawing of permafrost may in turn affect climate, for example, by releasing carbon dioxide or methane (Koven et al., 2011). It is therefore important to incorporate the carbon dynamics from an ecosystem model into the global climate model to investigate these complex feedbacks.

Conclusions

In this study, we estimated the FVC of quadrats using multispectral pictures, then upscaled first to a 30 m and then to a 1 km scale, using remote sensing data. We studied the spatial distribution of the FVC and the relationships between the FVC and LST in different types of frozen ground in two adjacent basins with different precipitation regimes, both located on the northeast ridge of the QTP. Our results indicated that the responses of alpine grassland in permafrost regions to climate warming were different at different stages of permafrost thawing and under different precipitation regimes. Climate warming might promote the growth of alpine grassland in some zones in semiarid basins and in all zones in semihumid basins. These differences should be considered when making proper mitigation and adaptation policies.

Acknowledgments

We would like to thank Mr. Naijie Li for his help in the field work, Mr. Shilong Ren for retrieving the fractional vegetation cover of the quadrats, and two anonymous reviewers for their constructive comments and suggestions. This study was supported by grants from the National Basic Research Program of China (2013CBA01807), the Strategic Priority Research Program (XDB030303), the China Special Fund for Meteorological Research in the Public Interest (GYHY201306017), and the National Natural Science Foundation of China (41271089).

References Cited

Barlage, M., and Zeng, X., 2004: The effects of observed fraction vegetation cover on the land surface climatology of the community land model. *Journal of Hydrometeorology*, 5: 823–830.

Baumann, F., He, J., Schmidt, K., Kühn, P., and Scholten, T., 2009: Pedogenesis, permafrost, and soil moisture as controlling factors for soil nitrogen and carbon contents across the Tibetan Plateau. *Global Change Biology*, 15, 3001–3017.

Du, M., Kawashima, S., Yonemura, S., Zhang, X., and Chen, S., 2004: Mutual influence between human activities and climate change in the Tibetan Plateau during recent years. *Global Planet Change*, 41: 241–249.

Harris, R. B., 2010: Rangeland degradation on the Qinghai-Tibetan plateau: a review of the evidence of its magnitude and causes. *Journal of Arid Environments,* 74: 1–12.

Jorgenson, T. M., Shur, Y. L., and Pullman, E. R., 2006: Abrupt increase in permafrost degradation in Arctic Alaska. *Geophysical Research Letters*, 33: L02503. http://dx.doi.org/10.1029/2005GL024960.

Li, J., Yu, S., Chen, J., Zhang, B., Wu, J., and Zhang, X., 2012: Modeling permafrost temperature distribution and analyzing zoning characteristics of permafrost in the source region of the Datong River. *Journal of China University of Mining & Technology*, 41(1): 145–152 (in Chinese with English abstract).

Li, S., and Cheng, G., 1996: Permafrost map on the Qinghai–Tibet Plateau (1:3 000 000). Lanzhou, China: Gansu Culture Press (in Chinese).

Karnieli, A., Agam, N., Pinker, R. T., Anderson, M., Imhoff, M. L., Gutman, G. G., Panov, N., and Goldberg, A., 2010: Use of NDVI and land surface temperature for drought assessment: merits and limitations. *Journal of Climate*, 23: 618–633.

Koven, C. D., Ringeval, B., Friedlingstein, P., Ciais, P., Cadule, P., Khvorostyanov, D., Krinner, G., and Tarnocai, C., 2011: Permafrost carbon-climate feedbacks accelerate global warming. *Proceedings of the National Academy of Sciences,* 108(36): 14769–14774.

Niu, L., Ye, B., Li, J., and Sheng, Y. 2011: Effect of permafrost degradation on hydrological processes in typical basins with various permafrost coverage in Western China. *Science China Earth Sciences.* http://dx.doi.org/10.1007/s11430-010-4073-1.

Qin, Y., Yi, S., Ren, S., Li, N., and Chen, J., 2014: Responses of typical grasslands in a semi-arid basin on the Qinghai-Tibetan Plateau to climate change and disturbances. *Environmental Earth Sciences*, 71: 1421–1431.

Schuur, E. A. G., Vogel, J. G., Crummer, K. G., Lee, H., Sickman, J. O., and Osterkamp, T. E., 2009: The effect of permafrost thaw on old carbon release and net carbon exchange from tundra. *Nature*, 459: 556–559.

Sheng, Y., Li, J., Wu, J., Ye, B., and Wang, J., 2010: Distribution patterns of permafrost in the upper area of Shule river with the application of GIS technique. *Journal of China University of Mining & Technology*, 39(1): 32–39 (in Chinese with English abstract).

Shur, Y. L., and Jorgenson, T. M., 2007: Patterns of permafrost formation and degradation in relation to climate and ecosystems. *Permafrost and Periglacial Processes,* 18: 7–19.

Waelbroeck, C., Monfray, P., Oechel, W. C., Hastings, S. J., and Vourlitis, G. L., 1997: The impact of permafrost thawing on the carbon dynamics of tundra. *Geophysical Research Letters,* 24(3): 229–232.

Wandwei, M., Steele, B., and Harris, R. B., 2013: Demographic responses of plateau pikas to vegetation cover and land use in the Tibet Autonomous Region, China. *Journal of Mammalogy*, 94: 1077–1086.

Wang, G., Li, Y., Wang, Y., and Wu, Q., 2008: Effects of permafrost thawing on vegetation and soil carbon pool losses on the Qinghai-Tibet Plateau. *China Geoderma,* 143: 143–152.

Wang, Z., Yang, G., Yi, S., Wu, Z., Guan, J., He, X., and Ye, B., 2012: Different response of vegetation to permafrost change in semi-arid and semi-humid regions in Qinghai-Tibetan Plateau. *Environmental Earth Sciences,* 66: 985–991.

Wu, Q., Lu, Z., and Liu, Y., 2006: Permafrost changes in the Tibetan Plateau. *Advances in Climate Change Research,* 2 (Supplement 1): 77–80.

Yang, M., Nelson, F. E., Shiklomanov, N. I., Guo, D., and Wan, G., 2010: Permafrost degradation and its environment effects on the Tibetan Plateau: a review of recent research. *Earth-Science Reviews,* 103: 31–44.

Yang, Z., Gao, J., Zhao, L., Xu, X., and Ouyang, H., 2013: Linking thaw depth with soil moisture and plant community composition: effects of permafrost degradation on alpine ecosystem on the Qinghai-Tibet Plateau: *Plant Soil*, 367: 687–700.

Yi, S., Zhou, Z., Ren, S., Xu, M., Qin, Y., Chen, S., and Ye, B., 2011: Effects of permafrost degradation on alpine grassland in a semi-arid basin on the Qinghai-Tibetan Plateau. *Environmental Research Letters,* 6. http://dx.doi.org/10.1088/1748-9326/6/4/045403.

Zhang, T., Osterkamp, T. E., and Stamnes, K., 1997: Effects of climate on the active layer and permafrost on the north slope of Alaska, U.S.A. *Permafrost and Periglacial Processes,* 8: 45–67.

Zhuang, Q., He, J., Lu, Y., Ji, L., Xiao, J., and Luo, T., 2010: Carbon dynamics of terrestrial ecosystems on the Tibetan Plateau during the 20th century: an analysis with a process-based biogeochemical model. *Global Ecology and Biogeography,* 19: 649–662.

MS accepted July 2014

Downloaded From: https://bioone.org/journals/Arctic,-Antarctic,-and-Alpine-Research on 15 Aug 2024
Terms of Use: https://bioone.org/terms-of-use